Journal of the Optical Society of Korea, Vol. 9, No. 4, December 2005, pp. 131-134

Absorption Coefficients for the Bound-to-continuum Transitions in a Biased Quantum-well Infrared Photodetector

Jeong-Woo Choe* and Hyung-Joon Hwang

Department of Physics, Kyung Hee University, Suwon 449-701, KOREA

(Received December 5, 2005 : revised December 15, 2005)

We have proposed a method to calculate the absorption coefficients for the bound-to-continuum transitions in a strong biased quantum-well infrared photodetector. We have applied this method to a manufactured sample of typical device parameters, and obtained good agreements with experiments. The absorption coefficients evaluated are up to 5,700/cm at some particular operating conditions. We have also been able to make a qualitative explanation for the bias dependence of response.

OCIS codes : 040.3060, 040.4200, 230.2090, 230.5160, 230.5590

I. INTRODUCTION

Over the past few years there has been significant progress in making Focal Plane Arrays (FPA) using Quantum Well Infrared Photodetectors (QWIP) to obtain the thermal image of objects [1-5]. Handheld QWIP cameras operating at 90 K with 1024×1024 pixels were introduced by Jet Propulsion Laboratory [1]. In these developments, the adoption of bound-to-continuum transitions to increase the detectivity (D^*) played a key role. Although this idea has resulted in a great experimental success, the theoretical understanding of the mechanism is not complete. QWIPs usually work in the photo-conductive mode under strong electric fields of about 30-50 kV/cm. However because of the conceptual difficulties of dealing with biased conditions, no one has been able to deal with QWIPs with these conditions in effect. Device design and the predictions for the response were made using the states for unbiased potentials. Enumerating a couple of these, O et. al evaluated the absorption coefficients for a Kastalsky- type detector using the Kronig-Penney model [6]. Liu studied the change of response with upper state position, especially when it crosses the barrier top [7]. Shechter and Shvartsman evaluated the limit values of absorption coefficients for a confined QWIP with artificial walls when the boundary walls become infinitely separated [8]. All these approaches assume unbiased potentials. When we apply a strong electric field to the structure, the upper states change dramatically from the unbiased ones, as roughly sketched in Fig. 1. Some scientists describe the Kronig bands slanting down along the potential and the hot electrons flow down along these bands. However considering the fact that the Kronig band widths are typically only a few meVs but the potential difference between the quantum wells is bigger than 100 meV under the usual operating conditions (for a 500 Å barrier, the difference becomes 150 meV when the electric field $F = 30$ kV/cm), it is not realistic to assume the states in different wells interact and form a band. In this situation it would be appropriate to regard the states above the barrier top as continuum states. The wave functions for the linear potential could be described by the Airy functions. In this work, we focus on evaluating the absorption coefficients for the bound-to-continuum transitions in a QWIP *under a bias*.

II. THEORY

In Fig. 2 (a), we depicted a photo-conductive type QWIP

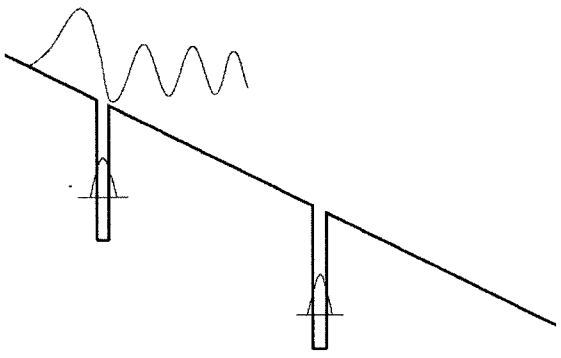

FIG. 1. A realistic modeling of a biased QWIP potential wave function. In the figure the electric field of 30 kV/cm had been assumed, which approximates a real operating condition.

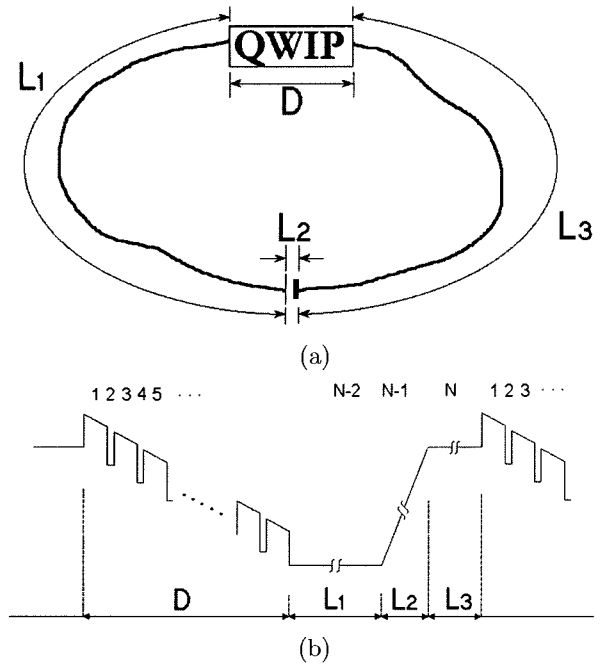

FIG. 2. (a) Schematic diagram for a detector in operation. (b) Approximate potential diagram in the growth direction for an electron of a QWIP with the periodic boundary condition.

under an operating condition. We explicitly displayed the connecting wires to an e.m.f. The mobile electrons circulate through the whole closed loop and the potentials they experience can be approximated as in Fig. 2 (b), adopting the periodic boundary conditions. In the figure, D stands for the length of the quantum well active region, L_1 and L_3 the length of wires including the heavily doped contacts, and L_2 the e.m.f. region where the potential increases to a higher level. Generally the connecting wires are much longer than the dimension of the quantum well (L_1, $L_2 \gg D$), and the specific values for them should not be important in the calculation. In fact, they are related to the normalization of wave functions and do not affect the final answer.

To estimate the absorption coefficient, we first need to determine the energy levels and the wave functions for a given potential. We use two different groups of basis functions for the flat and the tilted regions. In flat regions, we use the usual exponential functions (or the sinusoidal functions). In tilted regions, we use the first and the second kind of Airy functions the $Ai(\xi)$ and the $Bi(\xi)$,

$$\psi_j(x) = a_j\, Ai(\xi_j(x)) + b_j\, Bi(\xi_j(x)), \tag{1}$$

where x stands for the coordinate in the growth direction of a QWIP, ψ_j the electron wave function, and a_j and b_j the coefficients for the two independent basis functions in the region j ($j = 1, 2, \cdots, N$), and ξ_j's represent the dimensionless variables defined as [9]

$$\xi_j(x) = -(x - x_{0j}) / x_{\text{unit}} \tag{2}$$

with

$$x_{\text{unit}} = [\hbar^2 / (2 m_b e F)]^{\frac{1}{3}}. \tag{3}$$

In the above x_{0j} denotes the x coordinate of the point where the linear potential of region j (or the extension) becomes the total electron energy E, $\hbar$ the Planck constant, m_b the effective electron mass for the barrier region, e the electronic charge, and F the electric field strength. If we use the continuity of wave functions and their first derivatives (weighted with their effective masses) between the region j and $j+1$, we obtain 2N homogeneous equations in the 2N variables a_j's and b_j's (accompanying with the periodic boundary conditions) as in the following.

$$\begin{aligned} &a_1 Ai(\xi_1(x_1)) + b_1 Bi(\xi_1(x_1)) = a_2 + b_2, \\ &-a_1 k_F Ai'(\xi_1(x_1)) / m_b - b_1 k_F Bi'(\xi_1(x_1)) / m_b \\ &= a_2 k_2 / m_w - b_2 k_2 / m_w, \end{aligned} \tag{4}$$

$$\cdots$$

$$\begin{aligned} &a_N k_N \cos(k_N d_N) / m_w - b_N k_N \sin(k_N d_N) / m_w \\ &\quad = -a_1 k_F Ai'(\xi_1(0)) / m_b - b_1 k_F Bi'(\xi_1(0)) / m_b, \end{aligned}$$

where $k_F = 1 / x_{\text{unit}}$, and x_j ($j = 1, 2, \cdots, N$) denotes the x coordinate of the right end point, k_j the electron wave vector, and d_j the length of the potential region j. The prime denotes the differentiation with respect to ξ, and m_w is the effective electron mass in the well region. For the existence of a non-trivial set of solutions for a_j's and b_j's, we need to have

$$\det \mathrm{T} = 0, \tag{5}$$

with T denoting the collection of coefficients for a_j's and b_j's in a matrix form, i.e., $T_{11} = Ai(\xi_1(x_1))$, $T_{12} = Bi(\xi_1(x_1))$, $\cdots$, $T_{2N,2N} = -k_N \sin(k_N d_N) / m_w$, etc. The equation (5) serves as the deterministic equation to find the possible energies for a given potential. We may find the solutions of eq. (5) numerically, for example, using a commercial routine such as the International Mathematical and Statistical Library (IMSL). The non-trivial set of solutions found for a_j's and b_j's for a specific eigen-energy E (solutions of eq. (5)) will represent the corresponding wave function. After we determine the energy levels and the wave functions, the absorption coefficients are obtained from [7, 10]

$$\begin{aligned} \alpha = &\frac{\pi e^2}{c \epsilon_0 n_r \omega} n_e \sin^2\theta \sum_{E_n} \omega_{n0}^2 | < E_n | x | E_0 > |^2 \\ &\times \frac{\Gamma/2}{\pi [(E_n - E_0 - \hbar\omega)^2 + (\frac{\Gamma}{2})^2]} \end{aligned} \tag{6}$$

where c is the velocity, ω the angular frequency, θ the incidence angle of a light ray, and ϵ_0 the permittivity of vacuum, n_r the refractive index of medium, n_e the electron density, and $\omega_{n0} = (E_n - E_0)/\hbar$ with $|E_n>$ the exited states and $|E_0>$ the ground state of an electron. Γ represents the excited state energy level broadening due to the fluctuations of well widths, etc.

III. COMPARISON WITH EXPERIMENT

We now apply this method to a manufactured GaAs/AlGaAs QWIP sample of well width 40 Å, barrier thickness 500 Å, and Al composition 0.28. The sample is prepared in a multiple quantum-well structure with 25 periods of wells and barriers between the highly Si-doped contact layers with concentrations of 2×10^{18} /cm^3. The top and the bottom contact layers are 0.3㎛ and 0.5 μm thick, respectively. The center 20 Å of each well is also Si-doped with the same concentration as in the contacts. Taking the electric field strength of 50 kV/cm in the active region (which is the assumed value for the experiments presented in Fig. 3), and varying the normalization length $L = L_1 + L_2 + L_3$ in Fig. 2 from 10,000 Å to 300,000 Å, we have determined the possible energy levels that satisfy the eigenvalue equation (5). Consistent answers could be obtained when L is greater than 100,000 Å. The ground state energy was found invariably at 85.1 meV above the bottom of a well. The shape of ground state wave function has not changed from the unbiased ones. However the excited state wave functions have changed appreciably. The energy differences between the next neighboring eigen- states decrease as ~1/L when the normalization length L increases. The effective number of states included in the sum of eq. (6) increases as L.

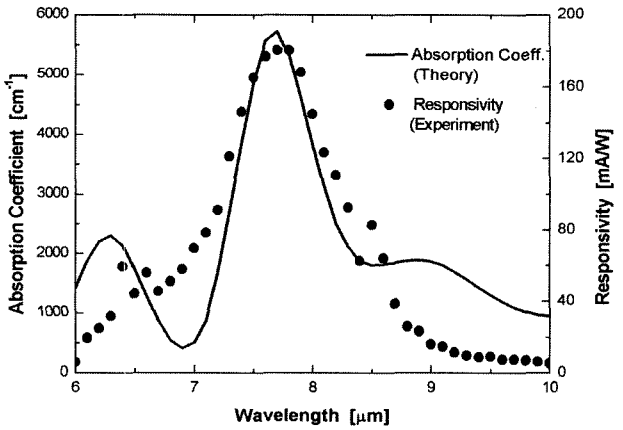

FIG. 3. Calculated spectral change of absorption coefficients (solid curve), and the measured spectral response for a sample (scattered data) with well width of 40 Å, barrier thickness of 500 Å, and barrier height of 195 meV. The electric field strength inside the structure was assumed to be 50 kV/cm.

On the other hand, the squared value of normalization coefficient for the excited level $|E_n>$ is proportional to 1/L. (the ground state wave function does not change). These observations ascertain that the final absorption coefficients do not depend on the particular choice of L.

We present the calculated spectral change of absorption coefficients in the case of $F = 50$ kV/cm in Fig. 3. In the figure the line broadening factor Γ of 10 meV has been used. We have also included the exchange interaction effects between the ground state electrons. The exchange interaction effect causes a downward shift of ground state energy level and demonstrates itself as a shift of response peak to a shorter wavelength [11]. For a 40 Å well with average doping density of 1×10^{18}/cm^3, the interaction energy was calculated to be ~12 meV, following the method presented earlier by the present author [12]. The calculated results agree well with the experimental responses. The absorption coefficient obtained reaches up to 5,700 /cm at the peak. However there are a couple of discrepancies between the calculated results and the experimental data, which need some explanations. One is that the calculated spectrum extends more to the long wavelength rather than showing a response cut off at the energy which is the difference between the ground state energy and the barrier top. This is mainly due to the fact that the calculated results are the absorption coefficients for a biased potential but the experimental data are for the spectral response. Unfortunately the absorption data for a biased QWIP is not available at the moment. For a biased potential there are eigen- states allowed even at the energy under the barrier top (the eigen-states become continuum states). Absorptions to these states are possible, but the electrons excited to these levels should have some difficulties in getting out of the barrier to contribute to photo-currents, resulting in a sharp decrease in the response. Second is that we see some bumps in the calculated spectrum, which do not show up explicitly in the experimental response. We may see a slight indication of response increase at the points where the calculation shows peaks, but not that distinctly predicted from the theory. There may be extra effects than the reason indicated in the above. For example, fluctuations of well widths may smear a sharp experimental peak, etc. But for the more exact explanations, we need further detailed studies.

Next we have applied our method to predict the bias dependence of response at one fixed wavelength. Fixing the wavelength of radiation at 7.7 μm, we have calculated the absorption coefficients at various electric field strengths. The results are presented in the Fig. 4. We can find the absorption coefficient first increases up to some maximum value as the electric field increases, and then decreases. The experimental results, as depicted in the same figure, agree with these predictions. However, since the experimental values were measured for the external bias voltages, but the calculation was done for the electric field strengths, the comparison should be taken only in the

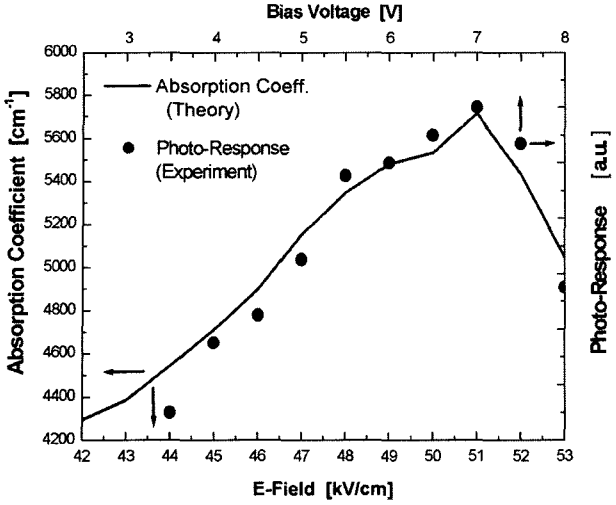

FIG. 4. Change of absorption coefficients with respect to the change in the electric field strengths (solid curve), and the bias dependence of responsivity (scattered data). The wavelength of incident radiation was fixed at 7.7 μm in both cases.

qualitative sense.

IV. CONCLUSION

We have proposed to use the *periodic* boundary conditions in calculating the absorption coefficients for the bound-to-continuum transition of a biased QWIP, which closely mimic the real operating conditions of a device. We have applied this method to a manufactured sample of typical device parameters and obtained good agreements between theories and experiments when the secondary effects such as the exchange interaction effects are included. The absorption coefficient obtained reaches up to 5,700/ cm at the peak. The bias dependence of response could be also explained from this scheme.

ACKNOWLEDGEMENTS

This work was supported by the Kyung Hee University Research Fund in 2003. The authors have benefited from helpful discussions with Dr. Suk-Joon Lee of Kyung Hee University.

*Corresponding author : jwchoe@khu.ac.kr

REFERENCES

[1] S. D. Gunapala, S. V. Bandara, J. K. Liu, C. J. Hill, S. B. Rafol, J. M. Mumolo, J. T. Trihn, M. Z. Tidrow, and P. D. LeVan, "Development of mid-wavelength and long-wavelength megapixel portable QWIP imaging cameras," *Infrared Physics & Technology*, vol. 47, pp. 67-75 (2005).

[2] E. Costard, P. Bois, X. Marcadet, and A. Nedelcu, "QWIP products and building blocks for high performance systems," Infrared *Physics & Technology*, vol.47, pp. 59-66 (2005).

[3] *A.* Rogalski, "Infrared detectors: status and trends," *Progress in Quantum Electronics* vol.27, pp. 59-210 (2003).

[4] C. J. Chen, K. K. Choi, W. H. Chang, and D. C. Tsui, *Appl. Phys. Lett.* vol. 72, pp. 7-9 (1998).

[5] K. K. Choi, *The Physics of Quantum Well Infrared Photodetectors* (World Scientific Publishing Co. Pte. Ltd., Singapore, 1997).

[6] Byungsung O, J.-W. Choe, M. H. Francombe, K. M. S. V. Bandara, and D. D. Coon, *Appl. Phys. Lett.* vol. 57, 503 (1990).

[7] H. C. Liu, *J. Appl. Phys.* 73, 3062 (1993).

[8] G. Shechter and L. D. Shvartsman, *Phys. Rev. B* vol. 58, 3941 (1998).

[9] L. D. Landau and E. M. Lifshitz, *Quantum Mechanics (Non. relativistic Theory)* 3rd Ed. (Pergamon, New York, 1977) pp. 75-76.

[10] S. L. Chuang, *Physics of Optoelectronic Devices* (John Willey & Sons Inc., New York, 1995), pp. 341-343.

[11] K. M. S. V. Bandara, D. D. Coon, Byungsung O, Y. F. Lin, and M. H. Francombe, *Appl. Phys. Lett.* vol. 53, 1931 (1988).

[12] J.-W. Choe, Byungsung O, K. M. S. V. Bandara, and D. D. Coon, *Appl. Phys. Lett.* vol. 56, 1679 (1990).